2011

Bottom-Up Synthesis of Gold Octahedra with Tailorable Hollow Features

Mark R. Langille
Northwestern University, MarkLangille2013@u.northwestern.edu

Michelle L. Personick
Northwestern University

Jian Zhang
University of Nebraska-Lincoln, jzhang3@unl.edu

Chad A. Mirkin
Northwestern University, chadnano@northwestern.edu

Published in *Journal of the American Chemical Society* 133:27 (2011), pp. 10414–10417; doi: 10.1021/ja204375d

Published online June 17, 2011.

Bottom-Up Synthesis of Gold Octahedra with Tailorable Hollow Features

Mark R. Langille, Michelle L. Personick, Jian Zhang, and Chad A. Mirkin

Department of Chemistry and International Institute for Nanotechnology, Northwestern University, 2145 Sheridan Road, Evanston, Illinois 60208, USA

Corresponding author — C. A. Mirkin, chadnano@northwestern.edu

Abstract

Gold octahedra with hollow features have been synthesized in high yield via the controlled overgrowth of preformed concave cube seeds. This Ag^+-assisted, seed-mediated synthesis allows for the average edge length of the octahedra and the size of the hollow features to be independently controlled. We propose that a high concentration of Ag^+ stabilizes the {111} facets of the octahedra through underpotential deposition while the rate of Au^+ reduction controls the dimensions of the hollow features. This synthesis represents a highly controllable bottom-up approach for the preparation of hollow gold nanostructures.

Noble metal nanostructures with hollow or porous features have been intensely investigated because they have markedly different properties when compared to their solid counterparts.[1, 2] The ability to control the dimensions of the hollow cavities within such noble metal nanoparticles allows for tailorable control of these unique plasmonic, catalytic, and electronic properties.[3-9] Consequently, hollow nanostructures have been used in numerous applications, functioning as nanoscale reactors for chemical reactions,[6-8] capsules for material containment,[10] substrates for generating surface-enhanced Raman scattering,[11-13] and for a variety of biomedical applications.[14-17] While there are many methods for generating nanostructures with hollow interiors,[1, 2] the vast majority of these procedures require a synthetic step where a sacrificial material is removed to generate the hollow features, as is the case for reactions based on galvanic replacements[18] and selective etchings.[19] The preparation of these structures could be simplified if a materials removal step was not required and a bottom-up, rather than a top-down, approach is utilized. Recently, there have been reports of bottom-up syntheses for hollow nanostructures, which include one-pot galvanic replacement reactions,[20, 21] electrochemical methods,[22, 23] and reactions that utilize diffusion processes or Kirkendall effects.[24] However, it can be difficult to control all of the architectural parameters of the particles produced in these syntheses, especially when compared to the bottom-up seed-mediated syntheses of solid Au nanostructures, which can be used to generate a variety of different-shaped particles (e.g., cubes,[25] octahedra,[26] rods,[27, 28] triangular nanoprisms,[29-31] and bipyramids[32]) in a highly controllable manner. Herein, we report a high yield Ag^+-assisted, seed-mediated method to prepare gold octahedra with hollow features. This bottom-up synthetic approach is highly tailorable as it allows for the dimensions of the octahedra and the size of the hollow cavities to be independently controlled, providing access to a large range of architectures.

The gold octahedra were synthesized by the controlled overgrowth of preformed concave cubic gold nanocrystal seeds. First, concave cubes of various edge lengths were prepared by literature methods (Figure S1 in the Supporting Information).[33] A growth solution was then prepared by consecutively adding 200 μL of 1.0 M HCl, 150 μL of 10 mM $HAuCl_4$, 150 μL of 10 mM $AgNO_3$, and 75 μL of 100 mM ascorbic acid (AA) to a 10 mL solution of 100 mM cetyltrimethylammonium chloride (CTAC). Note that the Au^{3+}:Ag^+:AA ratio in the growth solution was 1:1:5. The reaction was initiated by the addition of the concave cube seeds. The solution was gently mixed and left undisturbed overnight (Supporting Information).

Scanning electron microscopy (SEM) characterization of the reaction products seeded with concave cubes having an average edge length of 64 ± 10 nm indicates that the reaction produced octahedral gold nanoparticles in high yield (>90%; Figure 1A). The octahedra are highly monodisperse in terms of size (edge length: 100 ± 5 nm) and are often observed as hexagonally close packed arrays. The particles are bound by well-defined {111} facets and have sharp edges and corners. Interestingly, SEM images of the octahedra show that they have non-uniform contrast on their faces, having darker contrast near the tips and lighter contrast at the center of each face (Figure 1A inset). Analysis by angle-dependent scanning transmission electron microscopy (STEM) of a single Au octahedron also shows unexpected variations in contrast, however, it is consistent with the SEM images (Figures 1C and S2). Energy-dispersive X-ray spectroscopy (EDX) was used to determine that the areas of less contrast in the STEM images are due to an absence of Au (Figure S3). Taken together, these observations suggest that the octahedra contain hollow cavities. A model of such a particle would consist of an octahedral shell circumscribed about a concave cube core, with the tips of the concave cube located at the centers of the faces of the octahedron (Figure 1B). This model contains six hollow cavities located near the tips of the octahedron between the concave cube core and the outer octahedral shell, which correlates well with the contrast observed by electron microscopy.

The size of the octahedra can be easily controlled by seeding the growth solution with concave cubes of different edge lengths. Reactions seeded by concave cubes with average edge lengths of 21 ± 4, 37 ± 6, 78 ± 9, and 127 ± 16 nm yield octahe-

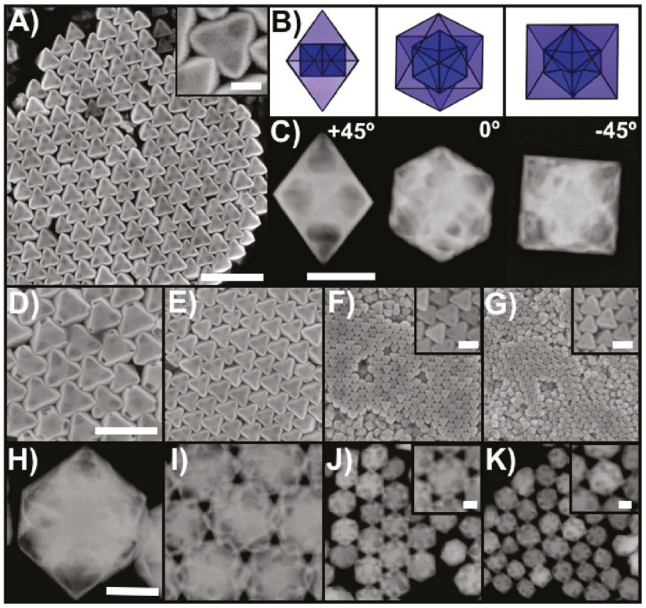

Figure 1. (**A**) Low-magnification SEM image of 100 nm edge length octahedra. Scale bar: 400 nm. Inset: high-magnification SEM image. Scale bar: 50 nm. (**B**) Model and (**C**) STEM images of a single hollow octahedron at different orientations (the substrate is tilted +45°, 0°, and −45°). Scale bar: 100 nm. (**D–G**) SEM and (**H–K**) STEM images of octahedra with average edge lengths of 206, 128, 54, and 41 nm, respectively. (D–G) Scale bars: 400 nm; insets, 50 nm. (H–K) Scale bars: 100 nm; insets, 20 nm.

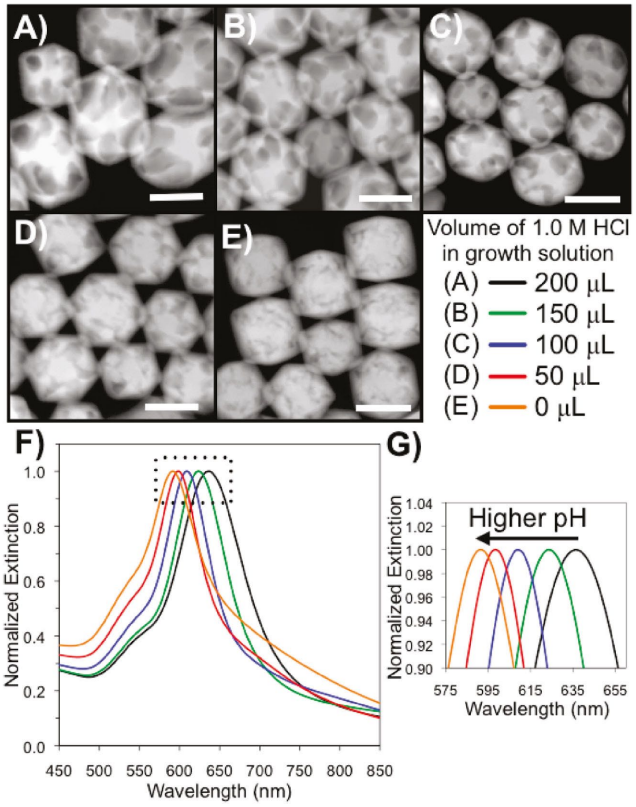

Figure 2. STEM images of 60 nm octahedra prepared in growth solutions containing (**A**) 200, (**B**) 150, (**C**) 100, (**D**) 50, and (**E**) 0 μL of 1.0 M HCl. Scale bars: 50 nm. (**F**) UV–vis spectra of the particles shown in (A–E) showing a gradual blue-shifting of their SPR with decreasing cavity size. (**G**) Magnified UV–vis spectra centered at the SPR maxima, corresponding to the region indicated with a box in (F).

dra with edge lengths of 41 ± 4, 54 ± 5, 128 ± 9, and 206 ± 21 nm, respectively. SEM (Figure 1D–G) and STEM (Figure 1H–K) images of the products confirm a high yield and the presence of hollow features, regardless of particle size. UV–vis spectroscopy was also used to characterize the particles. Typically, nanostructures with hollow interiors have a surface plasmon resonance (SPR) that is red-shifted from the corresponding solid particle.[2] Indeed, the 54 nm octahedra with hollow features have an SPR maximum at 605 nm, which is 25 nm red-shifted from that of similar-sized solid Au octahedra (Figure S4).[34]

Many of the plasmonic applications of noble metal nanostructures rely on the ability to tailor the SPR of a particle to a desired wavelength.[35-38] Other researchers have shown that the SPRs of hollow spherical gold nanoparticles are dependent on the size of their hollow cavity[3] and the thickness of the metal shell.[5] In our synthesis, we have found that the pH of the growth solution has a significant affect on product morphology. Interestingly, STEM characterization of products generated in growth solutions containing increasing amounts of HCl (from 0 to 200 μL of 1.0 M HCl yields growth solutions with pH values ranging from 4 to 2, respectively) indicate that the hollow features decrease in size at higher pH values (Figure 2). Remarkably, the shape and size of the octahedra remain largely unchanged upon varying the pH of the growth solution, as shown by SEM (Figure S5). As would be expected with decreasing cavity sizes,[3, 5] the SPR maximum gradually blue-shifts from 636 nm for the octahedra with the largest hollow features to 591 nm for the octahedra with the smallest hollow features. This same procedure can be used to control the size of the hollow features for larger octahedra as well (Figures S6 and S7). By adjusting the size of the concave cube seeds and the pH of the growth solution, the size of the octahedra and the size of the hollow cavities, respectively, can be independently controlled to yield a wide range of architectures and corresponding optical properties.

This seed-mediated synthesis is unusual in that it produces Au nanostructures with hollow features, rather than solid particles. To better understand the physical and chemical reasons for why these structures form, we investigated the importance of various reaction parameters. Intermediate particles between the concave cube seeds and the octahedra were obtained by reducing the amount of Au^{3+} added to the reaction, while maintaining a 1:1:5 ratio for Au^{3+}:Ag^{+}:AA (Figure 3). Because the amount of Au^{3+} is insufficient for the reaction to go to completion, the particles stop growing and it is possible to observe the progress of the reaction at various stages. SEM images of these particles indicate that growth occurs almost exclusively from the tips of the concave cubes, forming small {111}-faceted "plates" at the eight tips (Figure 3B). The plates increase in size laterally until they meet each other, forming the tips of an octahedron. We also investigated the importance of the shape of the concave cube seed particles. A variety of different-shaped Au nanostructures were prepared—{100}-faceted nanocubes, {730}-faceted tetrahexahedra, pseudo-spherical particles, and nanorods—according to literature methods and used as seeds, rather than the concave cubes, to initiate the reaction (see Supporting Information, Figure S8). SEM, TEM, and STEM images of the products of these reactions show that, regardless of seed morphology, {111}-faceted octahedra with hollow features are obtained (Figure S8). However, the octahedra generated from

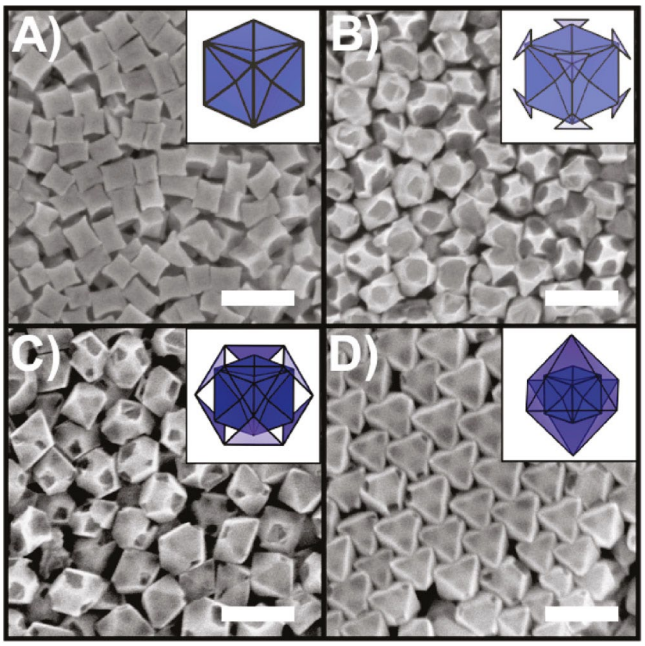

Figure 3. SEM images of (**A**) the concave cube seeds and the products of the octahedra reaction with (**B**) 50, (**C**) 100, and (**D**) 150 μL of a 10 mM $HAuCl_4$ solution. The Au^{3+}:Ag^+:AA ratio was maintained at 1:1:5 for all reactions. Scale bars: 100 nm.

these seeds are not produced in as high of a yield and the average size of the hollow cavities is smaller compared to when concave cube seeds are used. We believe that the high quality of the octahedra prepared from the concave cube seeds is due to the ability to prepare the concave cubes in high yield (>95%) and the fact that the concave faces of the cubes are ideal for generating structures with hollow cavities.

We hypothesize that these synthetic conditions favor the octahedral morphology due to the stabilization of {111} facets by Ag underpotential deposition (UPD).[39, 40] We recently reported the selective stabilization of Au {110}-faceted rhombic dodecahedra, {310}-faceted truncated ditetragonal prisms, and {720}-faceted concave cubes by using increasing concentrations of Ag^+ in synthetic conditions similar to those reported herein.[41] It was determined that the amount of Ag on the particles' surfaces has an excellent correlation with the number of exposed surface atoms for each respective facet, suggesting that up to a monolayer of Ag is deposited onto the most open facet for which there is sufficient Ag to cover. By depositing onto a specific facet, Ag inhibits the reduction of Au onto that surface and that facet is retained in the final structure. Interestingly, it was calculated that due to the hexagonally close packed arrangement of atoms on its surface, the low-index Au {111} facet has a greater number of exposed atoms for a given surface area (~1100 atoms per 100 nm^2) than the high-index {720} facet of the concave cubes (~1013 atoms per 100 nm^2).[41] Thus, it is expected that the stabilization of {111} facets by Ag UPD would require a higher Ag^+ concentration than is necessary to stabilize the {720} facets of the concave cubes. Indeed, a reaction seeded with preformed concave cubes conducted in a growth solution containing a Ag^+:Au^{3+} ratio of 1:5 yielded larger concave cubes (Figure S9). Then, with increasing ratios of Ag^+:Au^{3+}, the products display increasing surface areas of {111} facets until a ratio of 1:1 where the octahedra are fully formed (Figure S9). To quantitatively compare the silver coverage on the surface of the {720}-faceted concave cubes and the {111}-faceted octahedra, X-ray photoelectron spectroscopy (XPS) was used to determine the Ag:Au ratios for the two particle types (Figures S10 and S11). The results indicate that Ag coverage is slightly higher for the octahedra (Ag:Au = 0.30) than for the concave cubes (Ag:Au = 0.26). These values are also consistent with the trend predicted by calculated Ag:Au ratios for monolayer coverage of Ag on each facet type, assuming uniform signal from the top 1 nm of the sample (Figure S11). Taken together, these observations suggest that the very high Ag^+ concentration (Ag^+:Au^{3+} = 1:1) used in this synthesis is responsible for stabilizing the {111} facets of the octahedra, consistent with our previous work.[32, 33, 41]

These data also provide insight as to why the octahedra have hollow features. We believe that when the seed particles are added to the growth solution, which contains a high concentration of Ag^+, a dense (sub)monolayer coverage of Ag will be deposited onto the particles' surface by UPD. As the particles grow in size, Ag UPD will eventually stabilize a {111} facet because a {111} facet is able to support the densest Ag coverage and thus is most favorable at high Ag^+ concentrations. This leads to the formation of the {111}-faceted "plates" observed for incompletely grown particles (Figure 3B). At this point, Ag is inhibiting growth perpendicular to both the facets of the seed particles (which would be the {720} facets for the concave cubes) and the newly formed {111} facets. As a result, the most reactive site on the particles is at the edges of the {111}-faceted plates where there is a high degree of curvature. Therefore, the most rapid reduction of Au occurs onto the edges of the plates, which continue to grow until they ultimately meet each other, forming an octahedral shell around the seed particle. This type of growth is consistent with kinetically controlled reaction conditions in which slow reduction rates favor deposition onto the highest energy location of a growing nanostructure.[42-46] These kinetically controlled growth conditions are achieved by using a low solution pH (~2) and a high Ag^+ concentration, which together slow and inhibit the reduction of Au^+.[47] However, when the pH is raised to 4 by the omission of HCl, this preference for reduction onto the highest energy locations on the structure diminishes and the rate of growth perpendicular to the facets of the seed particle approaches the rate of growth parallel to the {111}-faceted plates, ultimately yielding an octahedral nanocrystal with smaller hollow features.

In conclusion, we have presented a high-yielding, Ag^+-assisted, seed-mediated synthesis of gold octahedra with hollow features. By introducing a high concentration of Ag^+ as an underpotential deposition agent in a Cl^--containing surfactant, the selective stabilization of {111} facets can be achieved to yield gold octahedra with hollow features. By controlling the size of the concave cube seeds and the solution pH, the size of both the octahedra and their hollow features can be independently controlled, allowing for the SPR of the particles to be easily tailored. The synthesis of these gold nanostructures with hollow features is notable because it is an entirely bottom-up procedure that does not require a conventional materials removal step, as is the case with galvanic replacements or selective etchants.

Acknowledgments — C.A.M. is grateful for an NSSEF Fellowship from the U.S. Department of Defense (DoD) and support from the

AFOSR. This work was supported in part by the MRSEC program of the National Science Foundation at the Materials Research Center of Northwestern University (DMR-0520513) and supported as part of the Non-Equilibrium Energy Research Center (NERC), an Energy Frontier Research Center funded by the U.S. Department of Energy, Office of Science, Office of Basic Energy Sciences (DE-SC0000989). The microscopy work was performed in the EPIC facility of NUANCE Center at Northwestern University. NUANCE Center is supported by NSF-NSEC, NSF-MRSEC, Keck Foundation, the State of Illinois, and Northwestern University. M.P. gratefully acknowledges support from the DoD through the National Defense Science & Engineering Graduate (NDSEG) Fellowship (32 CFR 168a).

Supporting Information

Experimental details; SEM of different-sized concave cube seeds; angle-dependent TEM and STEM images of a single particle; EDX data; UV–vis extinction spectra of different-sized octahedra with hollow features; SEM images of octahedra synthesized in different concentrations of HCl; SEM, STEM, and UV–vis spectra of large octahedra with different-sized hollow cavities; SEM images of different-shaped gold nanoparticles used as seeds; SEM, STEM, and TEM images of reaction products seeded by different-shaped particles; SEM images of products obtained at different Ag^{+}:Au^{3+} ratios; XPS spectra of the octahedra with hollow features; Plot comparing the experimental and calculated XPS Ag:Au ratios for concave cubes and octahedra—are presented following the **References**.

References

1. Lou, X. W.; Archer, L. A.; Yang, Z. C. *Adv. Mater.* 2008, 20, 3987
2. Cobley, C. M.; Xia, Y. N. *Mater. Sci. Eng.*, R 2010, 70, 44
3. Liang, H. P.; Wan, L. J.; Bai, C. L.; Jiang, L. *J. Phys. Chem. B* 2005, 109, 7795
4. Mahmoud, M. A.; El-Sayed, M. A. *J. Am. Chem. Soc.* 2010, 132, 12704
5. Schwartzberg, A. M.; Olson, T. Y.; Talley, C. E.; Zhang, J. Z. *J. Phys. Chem. B* 2006, 110, 19935
6. Mahmoud, M. A.; El-Sayed, M. A. *Nano Lett.* 2011, 11, 946
7. Zeng, J.; Zhang, Q.; Chen, J. Y.; Xia, Y. N. *Nano Lett.* 2010, 10, 30
8. Mahmoud, M. A.; Saira, F.; El-Sayed, M. A. *Nano Lett.* 2010, 10, 3764
9. Liang, H. P.; Zhang, H. M.; Hu, J. S.; Guo, Y. G.; Wan, L. J.; Bai, C. L. *Angew. Chem., Int. Ed.* 2004, 43, 1540
10. Yavuz, M. S.; Cheng, Y.; Chen, J.; Cobley, C. M.; Zhang, Q.; Rycenga, M.; Xie, J.; Kim, C.; Song, K. H.; Schwartz, A. G.; Wang, L. V.; Xia, Y. N. *Nat. Mater.* 2009, 8, 935
11. Mahmoud, M. A.; El-Sayed, M. A. *Nano Lett.* 2009, 9, 3025
12. Mahmoud, M. A.; Snyder, B.; El-Sayed, M. A. *J. Phys. Chem. C* 2010, 114, 7436
13. Oldenburg, S. J.; Westcott, S. L.; Averitt, R. D.; Halas, N. J. *J. Chem. Phys.* 1999, 111, 4729
14. Chen, J. Y.; Wang, D. L.; Xi, J. F.; Au, L.; Siekkinen, A.; Warsen, A.; Li, Z. Y.; Zhang, H.; Xia, Y. N.; Li, X. D. *Nano Lett.* 2007, 7, 1318
15. Zhang, J. Z. *J. Phys. Chem. Lett.* 2010, 1, 686
16. Timko, B. P.; Dvir, T.; Kohane, D. S. *Adv. Mater.* 2010, 22, 4925
17. An, K.; Hyeon, T. *Nano Today* 2009, 4, 359
18. Sun, Y. G.; Xia, Y. N. *Science* 2002, 298, 2176
19. Kim, S. W.; Kim, M.; Lee, W. Y.; Hyeon, T. *J. Am. Chem. Soc.* 2002, 124, 7642
20. Vasquez, Y.; Sra, A. K.; Schaak, R. E. *J. Am. Chem. Soc.* 2005, 127, 12504
21. Huang, X. Q.; Zhang, H. H.; Guo, C. Y.; Zhou, Z. Y.; Zheng, N. F. *Angew. Chem., Int. Ed.* 2009, 48, 4808
22. Peng, Z. M.; You, H. J.; Wu, J. B.; Yang, H. *Nano Lett.* 2010, 10, 1492
23. Huang, C. W.; Jiang, J. C.; Lu, M. Y.; Sun, L.; Meletis, E. I.; Hao, Y. W. *Nano Lett.* 2009, 9, 4297
24. Ben Moshe, A.; Markovich, G. *Chem. Mater.* 2011, 23, 1239
25. Sau, T. K.; Murphy, C. J. *J. Am. Chem. Soc.* 2004, 126, 8648
26. Xiang, Y. J.; Wu, X. C.; Liu, D. F.; Feng, L. L.; Zhang, K.; Chu, W. G.; Zhou, W. Y.; Xie, S. S. *J. Phys. Chem. C* 2008, 112, 3203
27. Jana, N. R.; Gearheart, L.; Murphy, C. J. *J. Phys. Chem. B* 2001, 105, 4065
28. Nikoobakht, B.; El-Sayed, M. A. *Chem. Mater.* 2003, 15, 1957
29. Millstone, J. E.; Park, S.; Shuford, K. L.; Qin, L. D.; Schatz, G. C.; Mirkin, C. A. *J. Am. Chem. Soc.* 2005, 127, 5312
30. Millstone, J. E.; Métraux, G. S.; Mirkin, C. A. *Adv. Funct. Mater.* 2006, 16, 1209
31. Millstone, J. E.; Wei, W.; Jones, M. R.; Yoo, H. J.; Mirkin, C. A. *Nano Lett.* 2008, 8, 2526
32. Personick, M. L.; Langille, M. R.; Zhang, J.; Harris, N.; Schatz, G. C.; Mirkin, C. A. *J. Am. Chem. Soc.* 2011, 133, 6170
33. Zhang, J.; Langille, M. R.; Personick, M. L.; Zhang, K.; Li, S. Y.; Mirkin, C. A. *J. Am. Chem. Soc.* 2010, 132, 14012
34. Li, C.; Shuford, K. L.; Park, Q. H.; Cai, W.; Li, Y.; Lee, E. J.; Cho, S. O. *Angew. Chem., Int. Ed.* 2007, 46, 3264
35. Jin, R. C.; Cao, Y. W.; Mirkin, C. A.; Kelly, K. L.; Schatz, G. C.; Zheng, J. G. *Science* 2001, 294, 1901
36. Jin, R. C.; Cao, Y. C.; Hao, E.; Métraux, G. S.; Schatz, G. C.; Mirkin, C. A. *Nature* 2003, 425, 487
37. Xue, C.; Mirkin, C. A. *Angew. Chem., Int. Ed.* 2007, 46, 2036
38. Xue, C.; Millstone, J. E.; Li, S.; Mirkin, C. A. *Angew. Chem., Int. Ed.* 2007, 48, 8436
39. Herrero, H.; Buller, L. J.; Abruña, H. D. *Chem. Rev.* 2001, 101, 1897
40. Magnussen, O. M. *Chem. Rev.* 2002, 102, 679
41. Personick, M. L.; Langille, M. R.; Zhang, J.; Mirkin, C. A., unpublished results.
42. Zhang, J.; Li, S. Z.; Wu, J. S.; Schatz, G. C.; Mirkin, C. A. *Angew. Chem., Int. Ed.* 2009, 48, 7787
43. Zhang, J.; Langille, M. R.; Mirkin, C. A. *J. Am. Chem. Soc.* 2010, 132, 12502
44. Washio, I.; Xiong, Y. J.; Yin, Y. D.; Xia, Y. N. *Adv. Mater.* 2006, 18, 1745
45. Langille, M. R.; Zhang, J.; Mirkin, C. A. *Angew. Chem., Int. Ed.* 2011, 50, 3543
46. Zhang, J., Langille, M. R., and Mirkin, C. A. *Nano Lett.* 2011, 11, 2495
47. Khan, M. M. T.; Martell, A. E. *J. Am. Chem. Soc.* 1968, 90, 3386